

Circulation effect: response of precipitation $\delta^{18}\text{O}$ to the ENSO cycle in monsoon regions of China

Ming Tan

Climate Dynamics

Observational, Theoretical and
Computational Research on the Climate
System

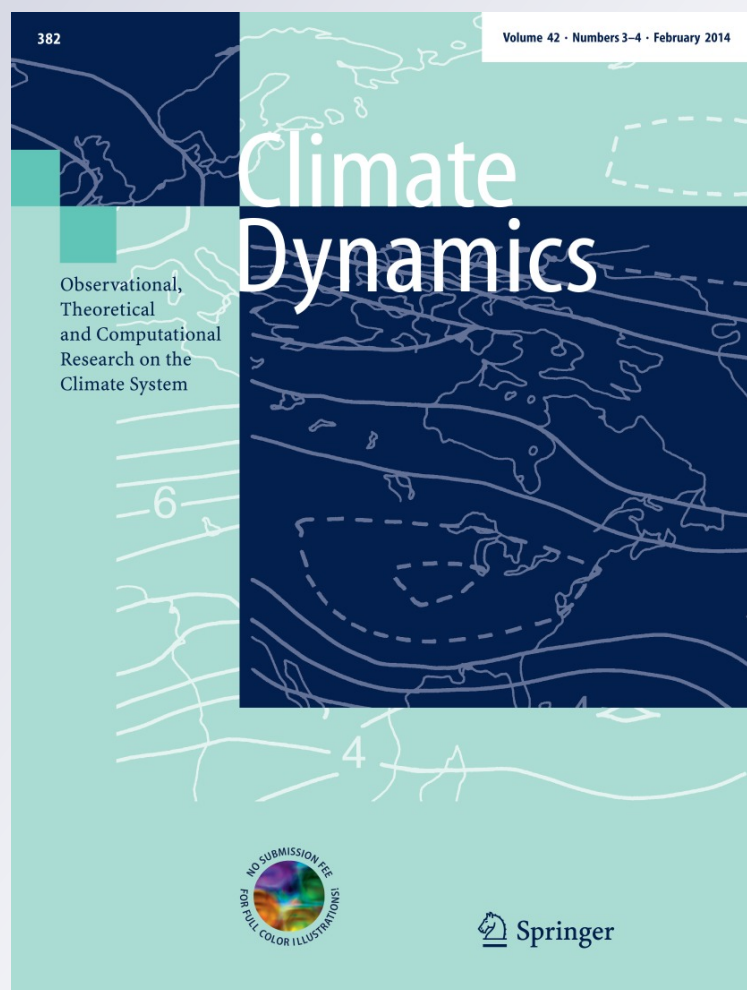
ISSN 0930-7575

Volume 42

Combined 3-4

Clim Dyn (2014) 42:1067-1077

DOI 10.1007/s00382-013-1732-x



Your article is protected by copyright and all rights are held exclusively by Springer-Verlag Berlin Heidelberg. This e-offprint is for personal use only and shall not be self-archived in electronic repositories. If you wish to self-archive your article, please use the accepted manuscript version for posting on your own website. You may further deposit the accepted manuscript version in any repository, provided it is only made publicly available 12 months after official publication or later and provided acknowledgement is given to the original source of publication and a link is inserted to the published article on Springer's website. The link must be accompanied by the following text: "The final publication is available at link.springer.com".

Circulation effect: response of precipitation $\delta^{18}\text{O}$ to the ENSO cycle in monsoon regions of China

Ming Tan

Received: 4 October 2012 / Accepted: 7 March 2013 / Published online: 21 March 2013
© Springer-Verlag Berlin Heidelberg 2013

Abstract Inter-annual variation in the ratio of ^{18}O to ^{16}O of precipitation ($\delta^{18}\text{O}_p$) in the monsoon regions of China (MRC, area approximately east of 100°E) has not yet been fully analyzed. Based on an analysis of the relationships between the time series of amount-weighted mean annual $\delta^{18}\text{O}$ in precipitation ($\delta^{18}\text{O}_w$) and meteorological variables such as temperature, precipitation as well as atmospheric/oceanic circulation indices, it is recognized that the El Niño-Southern Oscillation (ENSO) cycle appears to be the dominant control on the inter-annual variation in $\delta^{18}\text{O}_p$ in the MRC. Further analysis shows that the trade wind plays a role in governing $\delta^{18}\text{O}_w$ through affecting the intensity of the different summer monsoon circulations which are closely linked to the weakening (weaker than normal) and strengthening (stronger than normal) of the trade wind and gives the $\delta^{18}\text{O}_w$ different values at or over inter-annual timescales. The southwest monsoon (SWM) drives long-distance transport of water vapor from Indian Ocean to the MRC, and along this pathway increasing rainout leads to more negative $\delta^{18}\text{O}_w$ via Rayleigh distillation processes. In contrast, the southeast monsoon (SEM), which is consistent with the changes in the strength of the West Pacific subtropical high, drives short-distance water vapor transport from the West Pacific Ocean to the MRC and leads to less negative $\delta^{18}\text{O}_w$. Therefore, the $\delta^{18}\text{O}_w$ value directly reflects the differences in influence between the SWM, which is strong when the SE trade wind is strong, and the SEM, which is strong when the SE trade wind is weak.

In addition, the South China Sea Monsoon also transports local water vapor as well as plays a role in achieving the synchronization between the $\delta^{18}\text{O}_w$ and ENSO. The author thus terms the $\delta^{18}\text{O}_p$ rhythm in the MRC the “circulation effect”. In turn, the $\delta^{18}\text{O}_p$ variation in the MRC has the potential to provide information on atmospheric circulation and the signal of $\delta^{18}\text{O}_p$ recorded in natural archives can then be used to deduce a long-term behavior of the tropical climate system.

Keywords Circulation effect · Precipitation $\delta^{18}\text{O}$ · ENSO cycle · Trade wind · Monsoon regions of China

1 Introduction

Variations of the $^{18}\text{O}/^{16}\text{O}$ ratio ($\delta^{18}\text{O}$) in precipitation, tree rings, stalagmites, ice cores, corals and lake/ocean sediments have been providing atmosphere and climate information at regional and global scales. For instance, analyzing the $\delta^{18}\text{O}$ of precipitation ($\delta^{18}\text{O}_p$) collected from 13 monitoring stations across Russia between 1996 and 2000, Kurita et al. (2004) determined that, in Siberia, the westerly winds transport maritime air masses in winter, and in the summer moisture is supplied from the land surface. Well known examples of natural archives are the stalagmite oxygen isotope records ($\delta^{18}\text{O}_s$) from Hulu Cave, China (Wang et al. 2001) as well as other Chinese caves (e.g., Yuan et al. 2004; Johnson et al. 2006; Wang et al. 2008; Zhang et al. 2008; Cheng et al. 2009) which have been argued to be the East Asian paleomonsoon signal. However, it was the $\delta^{18}\text{O}_s$ from China that has aroused great debate worldwide over the past few years due to a lack of quantitative calibration. Maher (2008) inferred that, during Holocene, the Chinese speleothem isotope

M. Tan (✉)

Key Laboratory of Cenozoic Geology and Environment,
Institute of Geology and Geophysics, Chinese Academy
of Sciences, No.19 Beitucheng West Road, Chaoyang District,
Beijing 100029, China
e-mail: tanming@mail.iggcas.ac.cn

variations reflect changes not in rainfall amount but in rainfall source. Subsequently, Tan (2009) indicated that the most $\delta^{18}\text{O}_s$ series from the monsoon regions of China (MRC) record “the 1976–1977 climate shift of the Pacific Ocean” (Miller et al. 1994) and then named the changes in $\delta^{18}\text{O}_s$ from the MRC the “circulation effect” because it could reflect the variable ratio of the remote water vapor from the Indian Ocean and the local water vapor from the Pacific Ocean caused by the variability of large-scale atmospheric-oceanic circulation. Meanwhile, a simulation suggested that water isotope variability in Asian speleothems is linked to changes in landward water vapor transport rather than local precipitation (LeGrande and Schmidt 2009). Furthermore, Dayem et al. (2010) and Clemens et al. (2010) indicated that different precipitation sources and different pathways between the moisture source and the paleorecord site can partly cause the fluctuation of Chinese $\delta^{18}\text{O}_s$. And Clemens et al. (2010) also argued that the Chinese $\delta^{18}\text{O}_s$ reflect the combined influence of both summer monsoon circulation and winter temperature changes. Some models, however, show that the best interpretations of $\delta^{18}\text{O}_s$ appear to be site-specific and often regional in scale (e.g., Lewis et al. 2010). Recently, Maher and Thompson (2012) concluded that a possible driver of the Chinese $\delta^{18}\text{O}_s$ is precessional forcing of inter-hemispheric temperature gradients, and resultant shifts in the position and intensity of the subtropical pressure cells. These authors, without exception, suggest that the $\delta^{18}\text{O}_s$ is inherited from the $\delta^{18}\text{O}_p$. Therefore, a possible solution to these debates depends on understanding of the significance of the $\delta^{18}\text{O}_p$ in the MRC.

According to the zero-point energy theory (Einstein and Stern 1913), the light isotopes which possess higher zero-point energy diffuse or react faster than the heavy ones. Therefore H_2^{16}O requires less energy to vaporize than H_2^{18}O , as a result, the water vapor is depleted in ^{18}O whereas the residual liquid is enriched in ^{18}O . When water vapor condenses into liquid, H_2^{18}O preferentially enters the liquid, while H_2^{16}O is concentrated in the remaining vapor under constant temperature conditions. As an air mass moves from a warm region to a cold region, water vapor condenses and is removed as precipitation. The phenomenon that lower temperature causes precipitation to have lower $^{18}\text{O}/^{16}\text{O}$ ratio during the distillation processes was first observed by Dansgaard (1953) and later called the “temperature effect” (Dansgaard 1964). The above-mentioned principle also explains other important observations: $\delta^{18}\text{O}$ decreases with increasing precipitation rates due to reduced evaporation of liquid condensate, especially in convective-type precipitation events, which explains one type of the so-called “amount effect”. The amount effect refers to several kinds of processes, according to Risi et al. (2008), the re-evaporation of the falling rain and the diffusive exchanges with

the surrounding vapor, as well as the recycling of the sub cloud layer vapor feeding the convective system by convective fluxes. Seasonal changes in $\delta^{18}\text{O}_p$ resulting from the amount effect, first described by Dansgaard (1964), have been a starting point for isotope-related researches including those highlighting the amount effect in China (e.g., Araguás-Araguás et al. 1998; Tian et al. 2003; Yamanaka et al. 2004; Johnson and Ingram 2004). The amount effect has long been related to the main property of $\delta^{18}\text{O}_p$ in the regions affected strongly by summer monsoon. Supporting evidence is not only from the observational data, but also GCM simulations. For example, Vuille et al. (2005) investigated the influence of the Asian monsoon on $\delta^{18}\text{O}_p$ in the ECHAM-4 Atmospheric General Circulation Model; they show that variations in the amount of precipitation provide a first-order explanation for the $\delta^{18}\text{O}_p$. Meanwhile, they indicated that distillation processes during vapor transport, which increased rainout and depletion of heavy isotope upstream, may also lead to a significant monsoon rainfall- $\delta^{18}\text{O}$ relationship. This was later supported by simulations of $\delta^{18}\text{O}_p$ for the last glacial period (Pausata et al. 2011) and over a vast area of China (Lee et al. 2012).

However, two main points Dansgaard (1964) mentioned should be emphasized before using $\delta^{18}\text{O}_p$ as a tracer of precipitation amount. First, the development of the concept of the amount effect was derived from monthly and even synoptic timescales. Second, the amount effect was presented based on the hypotheses that raindrop evaporation and isotopic equilibrium fractionation tend to increase $\delta^{18}\text{O}$ in small amounts of rain. It is clear that an unchanged water source is a precondition for these assumptions. But in some areas, such as in the MRC the water vapor source and the transport paths greatly change in different seasons or different years due to oscillations in the atmospheric circulation. For example, based on back trajectory analysis with the HYSPLIT model, Zheng et al. (2009) indicated that the differences of $\delta^{18}\text{O}_p$ values were determined by different water vapor transport paths for Yunfu city (22°22′–23°19′N, 111°03′–112°31′E): relatively higher $\delta^{18}\text{O}_p$ values of the water vapor located in the South China Sea and the West Pacific Ocean, whereas relatively lower $\delta^{18}\text{O}_p$ values of the water vapor advected from the India Ocean and Bengal Gulf. In addition, according to isotope gradient analysis Liu et al. (2008, 2010) inferred that, for most regions of the MRC (except for a few areas in the west part of the MRC), the Pacific Ocean supplies the local water vapor enriched in ^{18}O and the Indian Ocean the distant water vapor depleted in ^{18}O .

Here, the author tries to explore the possible key role of ocean-atmosphere circulation patterns controlling inter-annual and longer-term variability of $\delta^{18}\text{O}_p$ in the MRC by examining observed amount-weighted mean annual $\delta^{18}\text{O}$ in precipitation data ($\delta^{18}\text{O}_w$), atmospheric/oceanic data as well as proxy data.

2 Data and methods

In this paper, comparative time series analysis is used to reveal the relationship between $\delta^{18}\text{O}_p$ and various climatic parameters. Mean monthly and annual $\delta^{18}\text{O}$ values of precipitation from all over the world have been archived as part of the Global Network for Isotopes in Precipitation (GNIP), which is governed by the International Atomic Energy Agency and the World Meteorological Organization. Besides $\delta^{18}\text{O}$ values of precipitation, the GNIP data also includes δD values of precipitation, precipitation amount, temperature and vapor pressure which are available at <http://www.iaea.org/>. The analytical uncertainty of isotope analyses is 0.11 ‰ for $\delta^{18}\text{O}$ and 1.3 ‰ for δD according to the GNIP report (<http://www-naweb.iaea.org/napc/ih/documents/userupdate/description/meet rept.htm>).

Oceanic and atmospheric data including the sea surface temperature anomaly (SSTA) and trade wind index (TWI) were obtained from the National Oceanic and Atmospheric Administration (NOAA), and available at <http://www.cpc.ncep.noaa.gov/data/indices/>. The SSTA of Niño3.4 (5°S–5°N, 170°W–120°W) has already been averaged over three-months and here it is further annually averaged as the Oceanic Niño Index (ONI). The TWI is defined at the 850 mb level within the equatorial Pacific regions (5°N–5°S) from 1979 to 2010. Two partitions (135E–180E/W and 175W–140W) of trade wind are combined here as a new TWI for comparison with other parameters. The data of difference of normalized sea level pressure (SLP) between Tahiti (148°W, 18°S) and Darwin (131°E, 12°S), which is called “Southern Oscillation Index” (SOI, from 1876 to 2011), are already organized by the Australian Government Bureau of Meteorology and obtained from <http://www.bom.gov.au/climate/current/soihtml.shtml>. The reanalysis datasets for drawing water vapor transport graphs are from the National Centers for Environmental Prediction (NCEP) and the National Center for Atmospheric Research (NCAR).

The southwest monsoon (SWM), which strongly affects the MRC, is a continuation of the Indian monsoon. Thus the strength of the SWM is here replaced with the India monsoon index which is usually represented by “All-India monsoon rainfall index” (AIMI). Combining rainfall from June 1 to September 30 the AIMI represents the Indian summer monsoon, and Indian area-weighted rainfall of 306 stations from 1871 to 2011 has been obtained from Indian Institute of Tropical Meteorology at <ftp://www.tropmet.res.in/pub/data/rain/iitm-regionrf.txt>.

The west Pacific subtropical high (WPSH) is one of the most important roles in governing the climate of the MRC (Zhou et al. 2009). Here, the index of westward extension of the WPSH (Lu and Ye 2010) and the index of the strength of the WPSH (Mu et al. 2002) are abbreviated as

WPSHI_w and WPSHI_s respectively. The reason for using the different indices of the WPSH is that the WPSHI_w extends forward into the twenty-first century and the WPSHI_s backward into the nineteenth century; however, in the intervening period, both are nearly equivalent. As a non-negligible water source for the MRC the South China Sea monsoon (SCSM) should be mentioned in the analysis, and the South China Sea monsoon index (SCSMI) is from Zheng et al. (2006). In addition, the precipitation data from meteorological stations in the MRC were downloaded from the China Meteorological Data Sharing Service System at <http://cdc.cma.gov.cn>.

The GNIP data for China consist of 30 sites, of which only Hong Kong possesses a dataset spanning more than 20 years. Using time series analysis, the author started with the Hong Kong site and subsequently applied the acquired knowledge to the whole MRC for further examination. For this purpose, the author recalculated the $\delta^{18}\text{O}_w$ for each year firstly based on the original monthly data, and subsequently excluding the yearly data which lacks data of two months or more. In addition, there is no oxygen isotope ratio data for July, August and October for 1982, but these can be infilled based on δD values of the same month and the local meteoric water line reconstructed according to the 411-month data series as a whole. Thus, a nearly continuous $\delta^{18}\text{O}_w$ dataset from 1980 to 2007 is obtained although there is a data gap of 2 years due to the absence of available data over several months in 2004 and 2005. The $\delta^{18}\text{O}_s$ data are available from NOAA website at <http://www.ncdc.noaa.gov/paleo/speleothem.html>.

3 Analysis and results

The time series of $\delta^{18}\text{O}_w$ in Hong Kong shows very poor correlation with the precipitation amount ($r = 0.05$, Fig. 1a) and the temperature ($r = -0.04$, not shown in the figure). The most notable relationship is that the peaks in precipitation are consistent with heavy peaks of the $\delta^{18}\text{O}_w$, i.e., in these years there were positive precipitation anomalies enriched in ^{18}O . Therefore, there must be some unknown relationship between the inter-annual changes in oxygen isotope ratio and climate variability. On annual time scales, most of the peak rainfall corresponds to heavier $\delta^{18}\text{O}_w$ in El Niño years as shown in Fig. 1a, hence a good relationship between the $\delta^{18}\text{O}_w$ and the El Niño–Southern Oscillation (ENSO) is expected. Actually the correlation coefficients between the $\delta^{18}\text{O}_w$ of Hong Kong and the ONI, SOI are 0.70 ($n = 26$) and -0.61 ($n = 26$) respectively, both significant at confidence levels higher than 99.9%. Meanwhile, the correlation coefficients between precipitation amount and the ONI and the SOI are 0.29 and -0.25 , respectively. In fact, some authors have

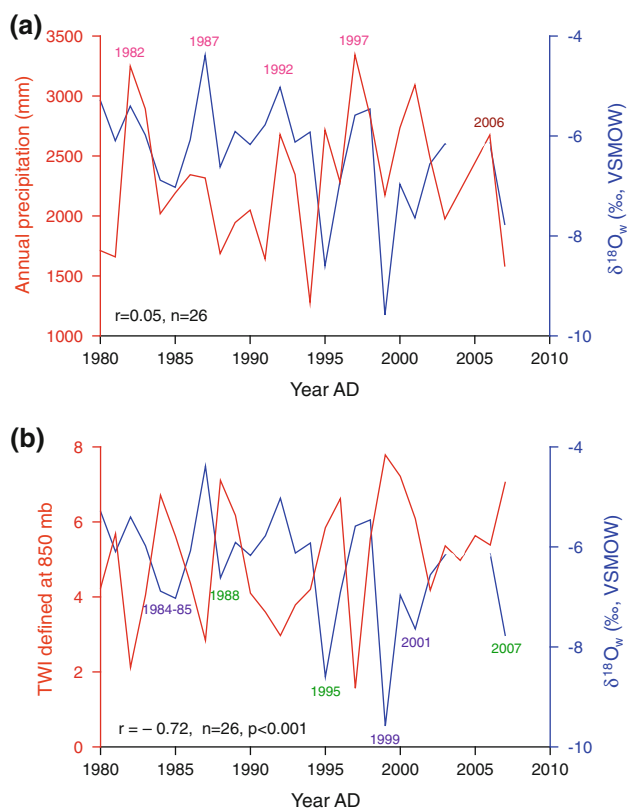


Fig. 1 **a** Comparison between annual precipitation amount (red curve) and $\delta^{18}\text{O}_w$ (amount-weighted annual mean, blue curve) for Kong Hong, data ranging from 1980 to 2007 with lack of data of 2004, 2005. **b** Comparison between the $\delta^{18}\text{O}_w$ of Hong Kong (blue curve) and the TWI (red curve, see text for details). The El Niño (pink) and La Niña (purple) years are labeled with the year in **a** and **b**, respectively, according to NOAA's assessment based on Niño 3.4 SSTA Niño Index (ONI). In 2006 El Niño occurred in the second half of the year (brown), and in 1988, 1995 and 2007 La Niña occurred in the second half of the year (green)

noted that the $\delta^{18}\text{O}_p$ in the Pearl River Delta or in Hong Kong has a statistically significant relationship with ENSO (Xue et al. 2007; Chen et al. 2010), but the underlying mechanism is not clear.

What is the mechanism controlling the changes in $\delta^{18}\text{O}_w$? In addition to temperature and amount effects, it could be either a change in the moisture source region or Rayleigh rainout processes. First, a “source effect”, i.e. variations in $\delta^{18}\text{O}_p$ affected by the isotopic composition of the ocean source water, should be taken into account. For example, the effect of relatively ^{18}O -enriched surface waters in the Atlantic Ocean, according to LeGrande and Schmidt (2006), results in isotopically heavier rainfall (reducing the bias from 0.6 to 0.3 ‰) over the Atlantic basin and surrounding land masses. Therefore, it is necessary to consider whether the sea water $\delta^{18}\text{O}$ of the Indian Ocean or the Pacific Ocean could significantly change when SST or evaporation intensity changes. However, as

has been revealed, sea water $\delta^{18}\text{O}$ was only on average 1 ‰ more positive during glacial episodes compared with interglacial episodes (Tracy et al. 1999). Thus, the impact of the seawater $\delta^{18}\text{O}$ on the precipitation $\delta^{18}\text{O}$ in recent decades is negligible compared with the rather large magnitude of inter-annual variation in $\delta^{18}\text{O}_p$ (see Fig. 1). Second, it is apparent that the SOI cannot be directly responsible for the ^{18}O -enriched increment of precipitation. The most likely scenario is that some atmospheric circulation plays a role of transporting ^{18}O -enriched or ^{18}O -depleted water vapor resulting in heavier or lighter values of $\delta^{18}\text{O}_w$ through a rainout process following Rayleigh distillation equation (Rayleigh 1896). This circulation, which should be associated with ENSO cycle, is certainly the trade wind that produces El Niño and La Niña by weakening and strengthening itself (Wyrski 1975).

The $\delta^{18}\text{O}_w$ of Hong Kong is compared with the TWI and the expected robust relationship between them is shown in Fig. 1b: correlation coefficient is $r = -0.72$, $n = 26$, $p < 0.001$. In addition, the light values of $\delta^{18}\text{O}_w$ correspond to La Niña years or the years in which La Niña occurred in the second half of the year. The most reasonable assumption for this phenomenon is that atmospheric ^{18}O is being depleted continuously by precipitation, increasing with water vapor transport distance (Siegenthaler 1979) in accordance with the principle of the Rayleigh rainout process.

Some studies emphasize $\delta^{18}\text{O}_p$ is influenced by a variety of factors (such as precipitation amount and temperature), and use multiple regressions to reveal which factor is more important. Based on the fact that the seasonal $\delta^{18}\text{O}_p$ pattern in Hong Kong consists of lower $\delta^{18}\text{O}$ values in the summer and higher values in the winter, Johnson and Ingram (2004) suggested that the dominant factor influencing stable isotopes in precipitation is the amount effect. To compare the relative importance of annual precipitation, temperature and trade wind (TWI) for the $\delta^{18}\text{O}_w$, multiple regressions are made here for Hong Kong using continuous annual data from 1983 to 2003 with the SPSS Statistics software. According to the results (Table 1), r^2 is 0.54, meaning that the sum of variance contribution of annual precipitation, temperature and trade wind is 54 %, and their resultant curve can basically describe the main variation of the

Table 1 Results of linear regression of $\delta^{18}\text{O}_w$ against climatic parameters for Hong Kong

Climate parameter	Standardized coefficient	Significance level	Partial correlation	r	r ²
Precipitation	-0.203	0.249	-0.278	0.735	0.540
Temperature	0.065	0.700	0.095		
Trade wind index	-0.748	0.000	-0.733		

Here std. coeff. relates algebraically to partial correlations

$\delta^{18}\text{O}_w$. The standardized coefficient and partial correlation are almost the same. The absolute value of the correlation coefficient shows the relative importance of each climate variable. Furthermore, given that only the trade wind passes the test of significance at $p < 0.001$ level, then it is clear that the $\delta^{18}\text{O}_w$ is primarily controlled by trade winds. Therefore, what we need to do is to further identify the provenance of the distant and the local vapor sources, as well as the mechanisms.

Based on the reanalysis datasets from the NCEP/NCAR, Tian et al. (2004) made a meteorological calculation of three main water vapor transport paths by using average summer water vapor transportation between 1958 and 1998 for the MRC. Their result shows that the water vapor flux (WVF) from Indian Ocean is $7,100\text{--}11,600 \text{ g cm}^{-1} \text{ hPa}^{-1} \text{ s}^{-1}$, from the South China Sea $4,200\text{--}7,600 \text{ g cm}^{-1} \text{ hPa}^{-1} \text{ s}^{-1}$ and from Pacific Ocean $2,500\text{--}7,500 \text{ g cm}^{-1} \text{ hPa}^{-1} \text{ s}^{-1}$. It is obvious that the WVF from Indian Ocean, which is transported by the SWM or sometimes referred to Indian monsoon, plays a dominant role in the transport of water vapor to the MRC (see the base map of water vapor transport in Fig. 6). Therefore, it is not surprising that the total of precipitation amount of the MRC has a positive relationship with that of India. Indeed, the relationship between them has high confidence level based on the observational data (Fig. 2).

Although the main changes in rainfall in India and the MRC seem similar, the forcing may be not quite the same. Figure 2 shows that, in India, droughts occur during El

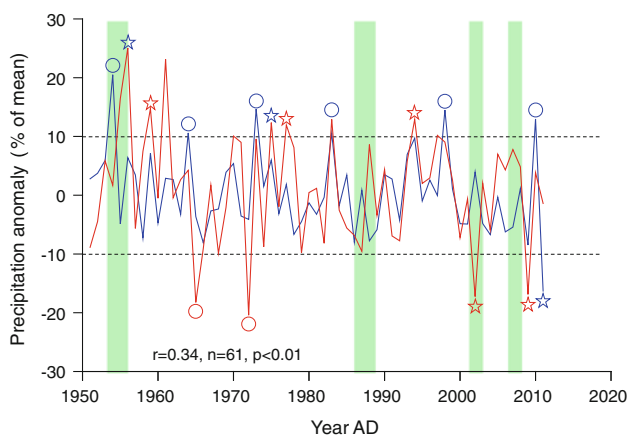


Fig. 2 Percentage of anomaly (reference period: 1981–2010) with respect to the average of precipitation amount of the MRC (blue line, 58 sites averaged without loss of data, annual mean) and that of total India (red line, 306 sites area-weighted, annual mean). Percentage more and less than 10 % is defined as flood and drought, respectively. El Niño years are marked with red stars and La Niña years blue stars. Red circle marks the years when the second half of the year is in the warm phase, and blue circle marks the years when the second half of the year is in the cold phase. Green columns indicate years when the changes between the precipitations of India and the MRC are in antiphase

Niño years or years when the warm phase takes place in the second half of year. In the MRC there are not many droughts but floods which occur in the years when the cold phase takes place in the second half of year, in which the WPSH extends westward in summer such as in 2010 and 1998 (Shen et al. 2011). Across the equator in summer the SE trade wind becomes the SWM over the Arabian Sea, which strongly affects the Indian subcontinent. Correlation analysis shows that the AIMI has a positive relation with the SOI at a confidence level greater than 99.9 %, implying that the higher the SOI and the stronger the trade wind or the AIMI, although the positive relationship between the Indian monsoon and the SOI seems intermittently weakened (Fig. 3). Actually, long before it was known that the Indian monsoon weakened during the El Niño period (Rasmusson and Carpenter 1983). On the other hand, the intensity of the SEM depends largely on the WPSH (Qiao et al. 2002), which mainly brings local water vapor from the West Pacific Ocean to the MRC leading to higher $\delta^{18}\text{O}_p$. Meanwhile, the SCSM is another driver transporting local ocean water from the South China Sea to the MRC (Zheng et al. 2009). Thus, it would make some sense to compare the WPSH_w and the SCSMI (Zheng et al. 2006). Comparative results show that they are out of phase at a confidence level higher than 99.9 %, and most heavy excursions of amount-weighted mean summer (JJA) precipitation $\delta^{18}\text{O}$ ($\delta^{18}\text{O}_{su}$) in Hong Kong occur concurrently with the intensity peaks of the two monsoons (Fig. 4).

The author here uses the WPSH_w (Lu and Ye 2010) to represent the SEM intensity for convenient analysis. The relationships shown in Fig. 4 indicate that the SEM and the SCSM are most likely responsible for the events of summer precipitation enriched in ^{18}O in Hong Kong (9 of 11), and

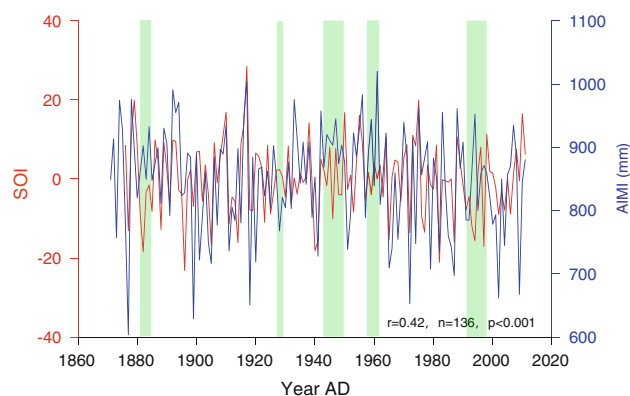


Fig. 3 Correlation between the SOI (red curve) and the intensity of the SWM (blue curve), which is usually inferred to be the Indian monsoon and sometimes represented by all-India average summer rainfall labeled as “All-India Monsoon Index” (AIMI). Here for consistency with the way in which the AIMI is calculated, an average SOI over June to September is used. Green columns indicate antiphases between the SOI and the AIMI

among them the SEM has slightly larger impact than the SCSM (5 of 9). Furthermore, because the relationship between the $\delta^{18}\text{O}_w$ and the $\delta^{18}\text{O}_{su}$ in Hong Kong is statistically significant at a high confidence level ($r = 0.68$, $n = 29$, $p < 0.001$), it could be acceptable to deduce the annual relationship using the summer relationship obtained here. Summarizing the above analysis, it is not temperature or precipitation but the circulation that markedly impacts the inter-annual variability of $\delta^{18}\text{O}_p$ in Hong Kong. Therefore, the term “circulation effect” (Tan 2009) could be used to describe the changes in $\delta^{18}\text{O}_p$ which originate from circulation fluctuations.

According to the Niño3.4 SSTA data from 1955 to 1998, Zhang et al. (2002) concluded that most cold phase years (16 out of 20) were followed by years when the SCSM was strong and subsequently El Niño occurred in autumn and winter (11 of 16). Meanwhile, most warm phase years (12 out of 15) were followed by the years when the SEM was strong and subsequently La Niña most likely occurred in autumn and winter (9 of 12). In light of these observations, it can be speculated that the reversed WPSHI_s lags the SOI by one year. Here the WPSHI_s is used to represent the intensity of the SEM, and the SOI represents the intensity of the trade wind because the TWI is available only since 1979. In fact, there is a statistically significant lagged relationship between the reversed WPSHI_s (Mu et al. 2002) and the SOI (Fig. 5).

In accordance with the above analysis, the relationship between the $\delta^{18}\text{O}_w$ in Hong Kong and various circulations could be fully described as follows:

1. The strength of the trade wind varies one-year ahead of the variation in the SCSM or the SEM. In the year when the trade wind is strong the local water vapor from the South China Sea or the West Pacific Ocean decreases while the distant water vapor depleted in ^{18}O from the Indian Ocean increases relatively, which results in the decrease of $\delta^{18}\text{O}_w$.
2. If the trade wind is abnormally weak in March, then the WPSH retreats from the South China Sea (SCS) earlier and further east. Later the westerly over the SCS is anomalously strong, so that the SCSM onsets early and is strong. Compared with normal years, water vapor originating from the SCS enriched in ^{18}O is transported northward, thus the $\delta^{18}\text{O}_w$ increases.
3. Subsequently, El Niño occurs in the period from autumn/winter (such as the typical event seen in 1982 and 1997) and even spring of the following year and leads to the strengthening and westward stretching of the WPSH during the summer (such as the typical event seen in 1983 and 1998), which carries the water vapor increment enriched in ^{18}O originating from the West Pacific Ocean to the inland and the $\delta^{18}\text{O}_w$ increases again.

The above analyses of processes and mechanisms describe, in a preliminary way, how and why the $\delta^{18}\text{O}_p$ in the MRC is affected by ENSO. Although the WPSH lags one year behind the major rhythm of the ENSO, the SCSM could adjust the synchronization of $\delta^{18}\text{O}_p$ to ENSO by resulting in the maximum values of $\delta^{18}\text{O}_p$. Wang et al. (2013) recently reveal that, by numerical experiment, the WPSH variation is primarily controlled by central Pacific cooling/warming and a positive atmosphere–ocean feedback between the WPSH and the Indo-Pacific warm pool oceans. This may answer the question of what makes the

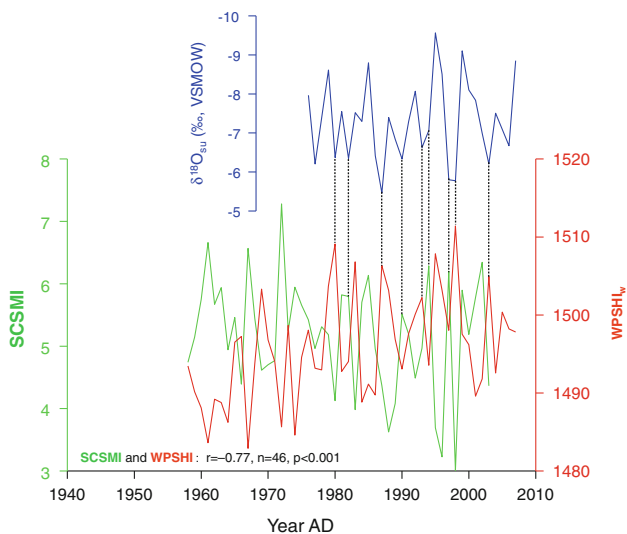


Fig. 4 Relations among the SCSMI (green curve, from Zheng et al. 2006), the WPSHI_w (red curve, from Lu and Ye 2010, used here to represent the SEM, see text for details) and the $\delta^{18}\text{O}_{su}$ of Hong Kong (see text for details). The dashed lines connect the extreme high values of $\delta^{18}\text{O}_{su}$ (axis reversed) and the intensity peaks of the WPSHI_w and the SCSMI, respectively

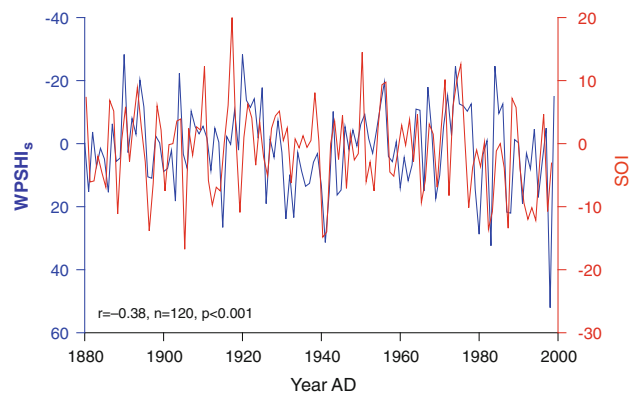


Fig. 5 Plot showing the lead-lag relationship between the SOI (red curve) and the reversed WPSHI_s (blue curve), here the former is one year ahead of the latter. In order to compare with the long time series of the SOI, the WPSHI_s series reconstructed by Mu et al. (2002) is used since it is longer than the WPSHI_w created by Lu and Ye (2010)

WPSH mostly strengthen during the summer of the El Niño decay year. However, it's not yet clear why the SCSM mostly strengthens in the El Niño onset year.

4 Further inferences

4.1 Spatial extent affected by ENSO

It is logical to presume that the circulation effect originating from weakening and strengthening of the trade wind should operate across a large spatial scale because the sphere of influence of atmospheric circulation should not be limited to a small region. However, this assumption needs to be confirmed.

Although most of the GNIP sites in China have only short annual time series, the results of the calculations are still meaningful if they meet the requirements of a statistically significant confidence level. Selecting GNIP sites in China possessing data covering continuous 5-year or longer time span, the author calculated the correlations between the $\delta^{18}\text{O}_w$ and the TWI, the precipitation amount, as well as the annual mean temperature. Ten sites meet the requirement of confidence level higher than 95 % (Table 2). Most commonly, the highest correlation exists between the TWI and the $\delta^{18}\text{O}_w$. A negative correlation exists between $\delta^{18}\text{O}_w$ and TWI in seven sites (circulation effects) and a negative correlation with precipitation amount only in three sites (amount effect). The spatial distribution of the time sequence further proves that the dominant rhythm of $\delta^{18}\text{O}_p$ in the MRC depends mainly on the change in the ratio of the water vapor transported by the SWM (remote) and the SEM (local), reflecting changes in the strength of the trade wind or the ENSO cycle (Fig. 6). It needs to be emphasized that, in the base map in Fig. 6 which shows the multi-year average of integrated water vapor transport, there appears to be no influence of the Pacific atmospheric circulation on the MRC but this is misleading. The role of atmospheric circulation over the Pacific Ocean is actually masked by the average state. The truth could be explained by the following analysis.

For further comprehension of the role of circulation in different climate scenarios, the author selected 1998 and 1999 as examples to compare the difference of the water vapor flux of the entire atmosphere during the summer of El Niño and La Niña years (according to their warm and cold phases in the first half of the year). As illustrated in Fig. 7, the SWM was stronger in 1999 than in 1998 (see the area circled by white dotted lines) because the trade wind was strong (see the area circled by white solid lines). On the other hand, the WPSH was strengthening and the SEM was stronger in 1998 than in 1999 (see the area circled by the pink solid line), leading to more water vapor transport

from the Pacific Ocean to the MRC in 1998 than in 1999 (see the area circled by the pink dotted line). This analysis of typical meteorological years further supports the conclusion presented above.

4.2 Different types of ENSO effects in Asia

Recent studies revealed that ENSO has an important effect on tree ring cellulose $\delta^{18}\text{O}$ in Laos (Xu et al. 2011) and Cambodia (Zhu et al. 2012), which corroborates the influence of ENSO on Southeast Asia with proxy evidence. The next question is “What makes the MRC different from other areas such as India and Southeast Asia that are also strongly affected by ENSO as firstly described by Walker (1918)?” Some proxy records from India confirm that the amount effect occurred prior to the instrumental period (e.g., Sinha et al. 2011a). However, areas which have multiple vapor sources mainly exhibit a circulation effect such as the MRC described above. Although both areas are influenced by the ENSO, the pathway is different: the monsoon region in India is directly controlled by the strength of the trade wind. But in the MRC, in addition to the trade wind, the monsoon region is also controlled by the modulation of the WPSH that is also driven by the ENSO (Zhou et al. 2009). However, the ENSO mentioned here is actually at different phases: the cold phase of ENSO associated with strong trade winds and the warm phase of ENSO associated with the strong WPSH. So, the WPSH is the key to understand a pronounced circulation effect occurring in the East Asian monsoon regions and some authors have been aware of this point, such as Maher and Thompson (2012). We are often confused by the similarity of $\delta^{18}\text{O}_s$ between India and China (such as described by Sinha et al. 2011b), whereas questions presented and analyzed in this paper may help to understand the differing causes of the isomorphic outcomes.

5 Long term behavior of the tropical climate system recorded in paleoproxies

GNIP can provide monitoring data covering only the past 50 years. Nevertheless, some natural archives such as tree rings or cave calcites could provide the opportunity to reconstruct the longer history of circulation changes as long as their $\delta^{18}\text{O}$ inherit $\delta^{18}\text{O}_p$. For example, Li et al. (2011a) reported that, in Shanxi Province in the MRC, variation in tree-ring cellulose $\delta^{18}\text{O}$ ($\delta^{18}\text{O}_t$) is similar to that of $\delta^{18}\text{O}_p$ during 1985–2002. Both $\delta^{18}\text{O}_t$ and $\delta^{18}\text{O}_p$ do not have any significant relationship with local temperature or precipitation, and they thus suggest that $\delta^{18}\text{O}_t$ as well as the $\delta^{18}\text{O}_p$ are not controlled by local temperature or precipitation, but are influenced by large-scale atmospheric

Table 2 Correlation coefficients and confidence levels between the $\delta^{18}\text{O}_w$ of the MRC, which have 5-year or more observed annual data from the GNIP, and the trade wind index, precipitation, temperature

Site	Years of observation	Correlation coefficients with trade wind index	Correlation coefficients with precipitation	Correlation coefficients with temperature
Ha'erbin 45°40'48"N, 126°37'12"E	5	-0.38	-0.64	-0.56
Baotou 40°40'12"N, 109°50'60"E	7	0.07	-0.44	-0.00
Tianjin 39°6'00"N, 117°10'01"E	7	-0.36	-0.37	-0.42
Shijiazhuang 38°1'60"N, 114°25'01"E	14	-0.30	-0.53, $p < 0.05$	-0.17
Zhengzhou 34°43'12"N, 113°39'00"E	5	-0.86, $p < 0.02$	-0.42	0.23
Chengdu 30°40'12"N, 104°1'12"E	8	-0.84, $p < 0.01$	-0.10	0.38
Lasa 29°41'60"N, 91°7'60"E	5	-0.75, $p < 0.05$	-0.12	-0.75, $p < 0.05$
Changsha 28°11'60"N, 113°4'01"E	5	-0.82, $p < 0.05$	0.11	Lack of data
Zunyi 27°41'60"N, 106°52'48"E	6	-0.54	-0.36	0.15
Guiyang 26°34'60"N, 106°43'01"E	5	-0.77, $p < 0.05$	-0.11	-0.45
Fuzhou 26°4'60"N, 119°16'59"E	6	-0.33	-0.15	-0.67
Guilin 25°4'12"N, 110°4'48"E	8	-0.63, $p < 0.05$	0.38	0.24
Kunming 25°1'00"N, 102°40'59"E	14	-0.45	-0.52, $p < 0.05$	-0.12
Hong Kong 22°18'36"N, 114°9'36"E	26	-0.72, $p < 0.001$	0.05	-0.04
Wulumuqi 43°46'48"N, 87°37'12"E	12	0.56	0.27	-0.08
Zhangye 38°55'48"N, 100°25'48"E	8	0.05	-0.30	-0.32
Hetian 37°7' 60"N, 79°55'60"E	5	0.79, $p < 0.05$	0.81, $p < 0.01$	-0.60
Yantai 37°31'48"N, 121°24'00"E	5	0.58	-0.86, $p < 0.02$	0.10
Nanjing 32°10'48"N, 118°10'48"E	5	0.15	-0.48	-0.24
Haikou 20°1'60"N, 110°20'60"E	6	0.23	0.34	-0.66

The boldface numbers highlight the confidence level higher than 95 %

circulation. Hence, they reconstruct the history of $\delta^{18}\text{O}_p$ linked to the ENSO since 1784 AD (Li et al. 2011b).

Based on monitoring at a cave in Guizhou Province in the MRC, Luo and Wang (2008) confirmed that the

precipitation is the main source of soil waters and cave drip waters and $\delta^{18}\text{O}$ values of the three types of water show similar fluctuations over time. At this site, the variance in $\delta^{18}\text{O}$ of drip water accounts only for a quarter of the

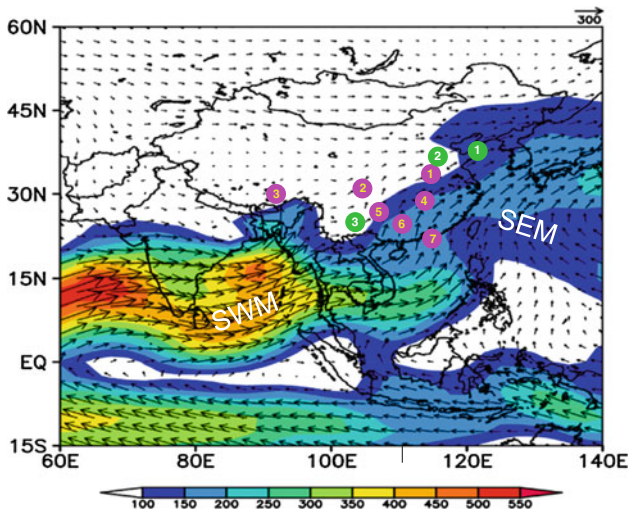


Fig. 6 Distribution of Chinese GNP sites possess circulation effect (pink) and amount effect (green). Base map shows the whole layer of integral water vapor transport vector of 1971–2000 average summer (June–August), unit: $g/(s\ cm)$. The pink dots are locations of 1 Zhengzhou, 2 Chengdu, 3 Lasa, 4 Changsha, 5 Guiyang, 6 Guilin and 7 Hong Kong. The Green dots are locations of 1 Yantai, 2 Shijiazhuang and 3 Kunming. The coloring indicates the magnitude of the moisture flux vector. SWM means the southwest monsoon and SEM the southeast monsoon

magnitude of that of precipitation due to mixing of precipitation events within the soil and ground-water system. A range of evidence to support this is presented by Fairchild and Baker (2012). Furthermore, a coupled atmosphere–ocean general circulation model suggests that simulated water isotope archives match well with those seen in speleothems as well as other natural sediments (LeGrande and Schmidt 2009). All of those studies suggest that cave process can transmit the signal of $\delta^{18}O_p$, so $\delta^{18}O_s$ reflects variability of circulation. In reality, some stalagmite records from the MRC have directly supplied convincing evidence that ENSO controls the fluctuation of $\delta^{18}O_s$. For example, the $\delta^{18}O_s$ of stalagmite HS4 (age controlled by annual layers) from Heshang Cave (Hu et al. 2008) has a strong negative relationship with the SOI (Fig. 8), which means that the stronger the trade wind the higher the ratio of vapor from the Indian ocean versus the Pacific ocean. Some authors (Aggarwal et al. 2012) recently found that, during El Niño events, increased precipitation in a warmer climate may occur with higher $\delta^{18}O$ values, which is contrary to previous assumptions made in interpreting proxy climate records in speleothems and other archives but consistent with the circulation effect. More ENSO-related cave records will continue to emerge if we adopt quantitative methods such as the “lumped parameter hydrological model” of Baker et al. (2012) to quantify the relative contributions of various factors to $\delta^{18}O_s$. Moreover, the most worthwhile thing to do is to identify how the

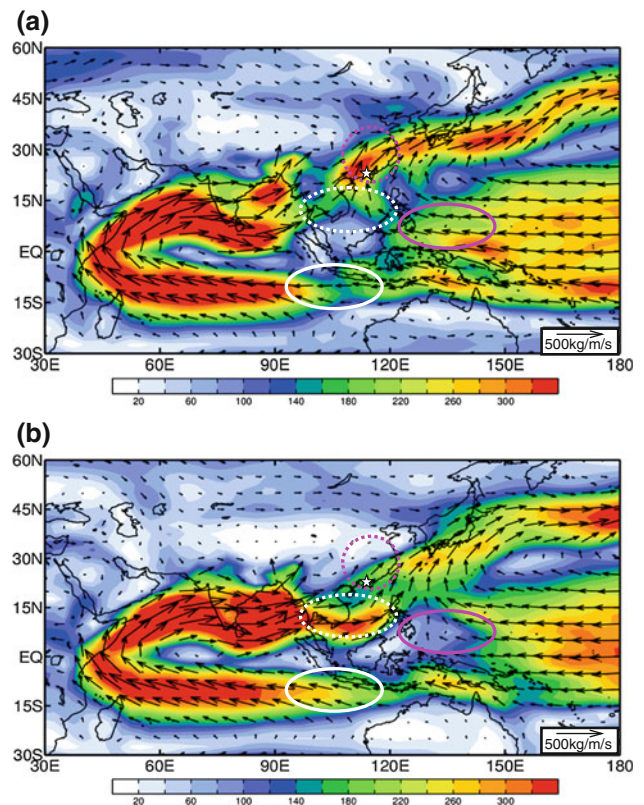


Fig. 7 a Total atmospheric water vapor flux for summer of 1999 based on the reanalysis monthly data from the NCEP and the NCAR, here the water vapor fluxes is from the surface to 300 hPa and different colors indicate the size of the entire water vapor flux (vector unit: $500\ kg\ m^{-1}\ s^{-1}$). **b** As **a** but for 1998. White or pink solid/dashed lines circle the compared regions for water vapor transporting over the two years (see text for details). White star is location of Hong Kong

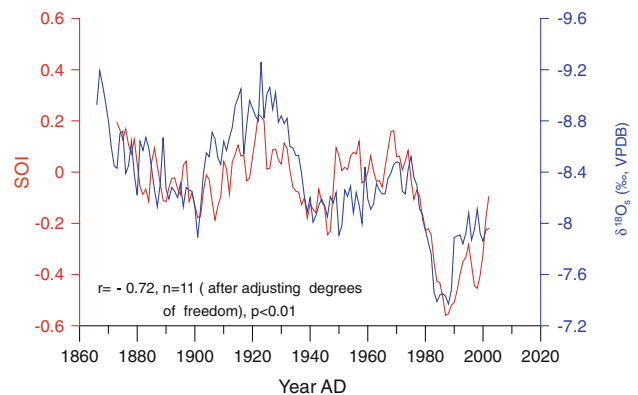


Fig. 8 Comparison and correlation between the SOI (red, 15-year running mean) and the stalagmite HS4 $\delta^{18}O$ sequence (blue). The SOI is high-frequency filtered to compare with the $\delta^{18}O_s$ which is smoothed due to mixing of precipitation events within the soil and ground-water system

$\delta^{18}O$ signal is distinctive of different sources (and the extent to which it is modified along pathways) through simultaneous cave monitoring over the MRC.

6 Conclusion and discussion

Summing up the time series analysis above, the so-called “circulation effect” can be expressed as follows: based on the Rayleigh distillation equation (Rayleigh 1896), the changes in the atmospheric–oceanic circulation can directly or indirectly affect the variation in the ratio of water vapor originating from distant oceans (becoming depleted in ^{18}O) and local ocean (relatively enriched in ^{18}O) to an observed site, resulting in the fluctuation in the $\delta^{18}\text{O}_p$ at this site. The rhythm of the $\delta^{18}\text{O}_p$ depends mainly on the variation in the atmospheric–oceanic circulation and can thus be termed as a circulation effect. At many sites in the MRC, the $\delta^{18}\text{O}_p$ reflects neither the amount effect nor strength of single summer monsoon but the intensity contrast between two summer monsoons—the southwest monsoon and the southeast monsoon, both of which are also related to ENSO. The author here provides evidence from certain datasets and some climate indices of a possible mechanism responsible for variations in $\delta^{18}\text{O}$ values. A useful next step would be to validate these mechanisms using isotope-enabled GCMs.

Acknowledgments Thanks to Ian Fairchild and Andy Baker for reviewing the manuscript and giving many encouragements and constructive suggestions. The author also thanks Zheng Bin for the SCSMI data, Lu Riyu for the WPSHI_w data, Wang Huijun for providing the map of Fig. 7 and Nan Sulan for providing base map of Fig. 6. Thanks to Duan Wuhui for assisting to build the multiple linear regression as well as Table 1. The author is very grateful to the three anonymous reviewers for their detailed and very helpful comments. This research was supported by CAS Strategic Priority Research Program (Grant XDA05080501), the NSFC (Grant 41030103) and the National Basic Research Program of China (Grant 2010CB950201).

References

- Aggarwal KP, Alduchov AO, Froehlich OK, Araguas-Araguas JL, Sturchio CN, Kurita N (2012) Stable isotopes in global precipitation: a unified based on atmospheric moisture residence time. *Geophys Res Lett* 39:L11705. doi:10.1029/2012GL051937
- Araguás-Araguás JL, Froehlich OK, Rozanski K (1998) Stable isotope composition of precipitation over southeast Asia. *J Geophys Res* 103(D22):28721–28742
- Baker A, Bradley C, Phipps SJ, Fischer M, Fairchild IJ, Fuller L, Spötl C, Azcurra C (2012) Millennial-length forward models and pseudoproxies of stalagmite $\delta^{18}\text{O}$: an example from NW Scotland. *Clim Past* 8:1153–1167
- Chen Z, Cheng J, Guo P, Lin Z, Zhang F (2010) Distribution characters and its control factors of stable isotope in precipitation over China. *Trans Atmos Sci* 33(6):667–679 (in Chinese with English abstract)
- Cheng H, Edwards RL, Broecker WS, Denton GH, Kong X, Wang Y, Zhang R, Wang X (2009) Ice age terminations. *Science* 326(5950):248–252
- Clemens SC, Prell WL, Sun Y (2010) Orbital-scale timing and mechanisms driving Late Pleistocene Indo–Asian summer monsoons: reinterpreting cave speleothem $\delta^{18}\text{O}$. *Paleoceanography* 25:PA4207. doi:10.1029/2010PA001926
- Dansgaard W (1953) The abundance of O^3 in atmospheric water and water vapour. *Tellus* 6:461–469
- Dansgaard W (1964) Stable isotopes in precipitation. *Tellus* 16:436–468
- Dayem KE, Molnar P, Battisti DS, Roe GH (2010) Lessons learned from oxygen isotopes in modern precipitation applied to interpretation of speleothem records of paleoclimate from eastern Asia. *Earth Planet Sci Lett* 295:219–230
- Einstein A, Stern O (1913) Einige Argumente für die Annahme einer molekularen Agitation beim absoluten Nullpunkt. *Ann Phys* 345(3):551–560
- Fairchild IJ, Baker A (2012) *Speleothem science: from process to past environments*. Wiley, Chichester, p 432
- Hu C, Henderson GM, Huang J, Xie S, Sun Y, Johnson KR (2008) Quantification of Holocene Asian monsoon rainfall from spatially separated cave records. *Earth Planet Sci Lett* 266(3–4):221–232
- Johnson KR, Ingram BL (2004) Spatial and temporal variability in the stable isotope systematics of modern precipitation in China: implications for paleoclimate reconstructions. *Earth Planet Sci Lett* 220:365–377
- Johnson KR, Ingram BL, Sharp DW, Zhang P (2006) East Asian summer monsoon variability during marine isotope stage 5 based on speleothem $\delta^{18}\text{O}$ records from Wanxiang Cave, central China. *Palaeogeogr Palaeoclimatol Palaeoecol* 236:5–19
- Kurita N, Yoshida N, Inoue G, Chayanova AE (2004) Modern isotope climatology of Russia: a first assessment. *J Geophys Res*. doi:10.1029/2003JD003404
- Lee JE, Risi C, Fung I, Worden J, Scheepmaker RA, Lintner B, Frankenberg C (2012) Asian monsoon hydrometeorology from TES and SCIAMACHY water vapor isotope measurements and LMDZ simulations: implications for speleothem climate record interpretation. *J Geophys Res* 117:D15112. doi:10.1029/2011JD017133
- LeGrande AN, Schmidt GA (2006) Global gridded data set of the oxygen isotopic composition in seawater. *Geophys Res Lett* 33:L12604. doi:10.1029/2006GL026011
- LeGrande AN, Schmidt GA (2009) Sources of Holocene variability of oxygen isotopes in paleoclimate archives. *Clim Past* 5:441–455
- Lewis SC, LeGrande AN, Kelley M, Schmidt GA (2010) Water vapour source impacts on oxygen isotope variability in tropical precipitation during Heinrich events. *Clim Past* 6:325–343
- Li Q, Nakatsuka T, Kawamura K, Liu Y, Song H (2011a) Regional hydro-climate and precipitation $\delta^{18}\text{O}$ revealed in tree-ring cellulose $\delta^{18}\text{O}$ from different tree species in semi-arid Northern China. *Chem Geol*. doi:10.1016/j.chemgeo.2011.01.004
- Li Q, Nakatsuka T, Kawamura K, Liu Y, Song H (2011b) Hydroclimate variability in the North China Plain and its link with El Niño–Southern Oscillation since 1784 A.D.: insights from tree-ring cellulose $\delta^{18}\text{O}$. *J Geophys Res* 116:D22106. doi:10.1029/2011JD015987
- Liu J, Song X, Yuan G, Sun X, Liu X, Wang Z, Wang S (2008) Stable isotopes of summer monsoonal precipitation in southern China and the moisture sources evidence from $\delta^{18}\text{O}$ signature. *J Geogr Sci* 18:155–165
- Liu J, Song X, Yuan G, Sun X, Liu X, Wang S (2010) Characteristics of $\delta^{18}\text{O}$ in precipitation over Eastern Monsoon China and the water vapor sources. *Chin Sci Bull* 55:200–211
- Lu R, Ye H (2010) Inter-annual and seasonal changes of the West Pacific subtropical high. In: He J, Qi L, Zhang R (eds) *The progress and application of the new research on the Western Pacific subtropical high*. Meteorological Press, Beijing (in Chinese with English abstract)
- Luo W, Wang S (2008) Oxygen isotope signals of precipitation-soil water-drip water and its implications in Liangfeng Cave of Guizhou, China. *Chin Sci Bull* 53:3364–3370

- Maher BA (2008) Holocene variability of the East Asian summer monsoon from Chinese cave records: a re-assessment. *Holocene* 18:861–866
- Maher BA, Thompson R (2012) Oxygen isotopes from Chinese caves: records not of monsoon rainfall but of circulation regime. *J Quat Sci*. doi:10.1002/jqs.2553
- Miller AJ, Cayan DR, Barnett TP, Graham NE, Oberhuber JM (1994) The 1976–1977 climate shift of the Pacific Ocean. *Oceanography* 7:21–26
- Mu Q, Wang S, Zhu J, Gong D (2002) Variations of Western Pacific Subtropical High in summer during the last hundred years. *Chin J Atmos Sci* 25:787–797
- Pausata FSR, Battisti DS, Nisancioglu KH, Bitz CM (2011) Chinese stalagmite $\delta^{18}\text{O}$ controlled by changes in the Indian monsoon during a simulated Heinrich event. *Nat Geosci* 4:474–480
- Qiao Y, Chen L, Zhang Q (2002) The definition of East Asian monsoon indices and their relationship to climate in China. *Chin J Atmos Sci* 26(1):69–82 (in Chinese with English abstract)
- Rasmusson EM, Carpenter TH (1983) The relationship between Eastern equatorial Pacific sea surface temperatures and rainfall over India and Sri Lanka. *Mon Wea Rev* 111:517–528
- Rayleigh JWS (1896) Theoretical considerations respecting the separation of gases by diffusion and similar processes. *Philos Mag* 42:493–498
- Risi C, Bony S, Vimeux F (2008) Influence of convective processes on the isotopic composition ($\delta^{18}\text{O}$ and δD) of precipitation and water vapor in the tropics: 2. physical interpretation of the amount effect. *J Geophys Res* 113:D19306. doi:10.1029/2008JD009943
- Shen H, Kuang Y, Zi L (2011) Genesis of 2012 storm–flood in Yangtze river basin and its comparison with 1998 flood. *Yangtze River* 42(6):11–14 (in Chinese with English abstract)
- Siegenthaler U (1979) Stable hydrogen and oxygen isotopes in the water cycle. In: Jäger E, Hunziker JC (eds) *Lectures in isotope geology*. Springer, Berlin, pp 264–273
- Sinha A, Berkelhammer M, Stott L, Mudelsee M, Cheng H, Biswas J (2011a) The leading mode of Indian Summer Monsoon precipitation variability during the last millennium. *Geophys Res Lett* 38:L15703. doi:10.1029/2011GL047713
- Sinha A, Stott L, Berkelhammer M, Cheng H, Edwards RL, Buckley B, Aldenderfer M, Mudelsee M (2011b) A global context for mega droughts in monsoon Asia during the past millennium. *Quatern Sci Rev* 30:47–62
- Tan M (2009) Circulation effect: climatic significance of the short term variability of the oxygen isotopes in stalagmites from monsoonal China. *Quat Sci* 29(5):851–862 (in Chinese with English abstract)
- Tian L, Yao T, Schuster PF, White JWC, Ichiyana K, Pendall E, Pu J, Yu W (2003) Oxygen-18 concentrations in recent precipitation and ice cores on the Tibetan Plateau. *J Geophys Res* 108(D9):4293. doi:10.1029/2002JD002173
- Tian H, Guo P, Lu W (2004) Characteristics of vapor inflow corridors related to summer rainfall in China and impact factors. *J Trop Meteorol* 20:401–408 (in Chinese with English abstract)
- Tracy AM, David WL, Howard JS (1999) Glacial–interglacial changes in subantarctic sea surface temperature and $\delta^{18}\text{O}$ -water using foraminiferal Mg. *Earth Planet Sci Lett* 170(4):417–432
- Vuille M, Werner M, Bradley RS, Keimig F (2005) Stable isotopes in precipitation in the Asian monsoon region. *J Geophys Res* 110:D23108. doi:10.1029/2005JD006022
- Walker GT (1918) Correlation in seasonal variation of weather. *Q J R Meteorol Soc* 44:223–224
- Wang Y, Cheng H, Edwards RL, An Z, Wu J, Shen C, Dorale JA (2001) High-resolution absolute-dated Late Pleistocene monsoon record from Hulu cave, China. *Science* 294:2345–2348
- Wang Y, Cheng H, Edwards RL, Kong X, Shao X, Chen S, Wu J, Jiang X, Wang X, An Z (2008) Millennial- and orbital-scale changes in the East Asian monsoon over the past 224,000 years. *Nature* 45:1090–1093
- Wang B, Xiang B, Lee JY (2013) Subtropical high predictability establishes a promising way for monsoon and tropical storm predictions. *Proceedings of the National Academy of Sciences*. doi:10.1073/pnas.1214626110PNAS January 22, 2013 201214626
- Wyrki K (1975) El Nino—the dynamic response of equatorial Pacific ocean to the atmospheric forcing. *J Phys Oceanogr* 5:572–584
- Xu C, Sano M, Nakatsuka T (2011) Tree ring cellulose $\delta^{18}\text{O}$ of *Fokienia hodginsii* in northern Laos: a promising proxy to reconstruct ENSO? *J Geophys Res* 116:D24109. doi:10.1029/2011JD016694
- Xue J, Zhong W, Zhao Y (2007) Variations of $\delta^{18}\text{O}$ in precipitation in the Zhujiang (Pearl) river delta and its relationship with ENSO event. *Sci Geogr Sin* 27(6):825–830 (in Chinese with English abstract)
- Yamanaka T, Shimada J, Hamada Y, Tanaka T, Yang Y, Zhang W, Hu C (2004) Hydrogen and oxygen isotopes in precipitation in the northern part of the North China Plain: climatology and inter-storm variability. *Hydrol Process* 18:2211–2222 (Special issue: water crises and hydrology in North China)
- Yuan D, Cheng H, Edwards RL, Dykoski CA, Keelly MJ, Zhang M, Qing J, Lin Y, Wang Y, Wu J, Dorale JA, An Z, Cai Y (2004) Timing, duration, and transitions of the last interglacial Asian monsoon. *Science* 304:575–578
- Zhang X, Li J, Wang D (2002) Research on relationship between subsurface sea temperature in tropical area and SCS summer monsoon. *Acta Meteorol Sin* 60:156–163 (in Chinese with English abstract)
- Zhang P, Cheng H, Lawrence RE, Chen F, Wang Y, Yang X, Liu J, Tan M, Wang X, Liu J, An C, Dai Z, Zhou J, Zhang D, Jia J, Jin L, Johnson RK (2008) A test of climate, Sun, and culture relationships from an 1810-year Chinese cave record. *Science* 322:940–942
- Zheng B, Gu D, Li C (2006) Differences of South China Sea summer monsoon derived by NCEP and ECMWF reanalysis data. *J Trop Meteorol* 12(2):197–200
- Zheng Y, Zhong W, Peng X, Xue J, Zhao Y, Ma Q, Cai Y (2009) Correlation of $\delta^{18}\text{O}$ in precipitation and moisture sources at Yunfu, Western Guangdong Province, China. *Environ Sci* 30(3):637–643 (in Chinese with English abstract)
- Zhou T, Yu R, Zhang J, Drange H, Cassou C, Deser C, Hodson DLR, Sanchez-Gomez E, Li J, Keenlyside N, Xin X, Okumura Y (2009) Why the Western Pacific subtropical high has extended Westward since the Late 1970s. *J Clim* 22:2199–2215
- Zhu M, Stott L, Buckley B, Yoshimura K, Ra K (2012) Indo-Pacific warm pool convection and ENSO since 1867 derived from Cambodian pine tree cellulose oxygen isotopes. *J Geophys Res* 117:D11307. doi:10.1029/2011JD017198